The Journal of Neuroscience, August 1987, 7(8): 2423–2432

Distribution of Potassium Conductance in Mammalian Müller (Glial) Cells: A Comparative Study

Eric A. Newman

Eye Research Institute of Retina Foundation, Boston, Massachusetts 02114

The distribution of K^+ conductance across the surface of retinal Müller cells was determined in 5 mammalian species—rabbit, guinea pig, mouse, owl monkey, and cat—and in tiger salamander. Potassium conductance was measured by monitoring cell depolarizations evoked by focal ejections of a high-K^+ solution onto the surface of freshly dissociated cells. This technique measured the total K^+ conductance of a given cell region (regional conductance), i.e., the specific K^+ conductance *times* the total surface area in that region. In mammalian species with avascular retinas (rabbit, guinea pig), the regional K^+ conductance within the middle portion of the cell was only a fraction (10.6–28.9%) of the endfoot conductance, while the conductance of the distal (photoreceptor) end of the cell was approximately half (41.2–49.8%) the endfoot conductance. In 2 species with vascularized retinas (mouse and owl monkey), by contrast, the regional K^+ conductance within the middle portion of the cell was as large as 125.5–129.8% of the endfoot conductance. In these cells the K^+ conductance of the distal end was 68.3–82.9% of the endfoot value. In cat, a third vascularized species, the K^+ conductance was highest (187.1% of the endfoot value) at the distal end of the cell. In tiger salamander, which has an avascular retina, the regional K^+ conductance of all regions distal to the endfoot was only 2.4–15.7% of the endfoot value. Differences in the distributions of regional K^+ conductance observed in the 6 species raise the possibility that in vascularized mammalian retinas, the high-K^+ conductance of the middle portion of Müller cells is associated with retinal blood vessels. The results are consistent with the hypothesis that, in avascular species, Müller cells aid in regulating extracellular K^+ levels by transferring (siphoning) excess K^+ principally into the vitreous humor, while in at least some vascularized species (mouse, monkey), excess K^+ is transferred by Müller cells into retinal capillaries, as well as into the vitreous.

Glial cells of the vertebrate CNS are almost exclusively permeable to potassium (Orkand, 1977; Kettenmann et al., 1983; Walz et al., 1984; Newman, 1985a). In some types of glial cells, it has been shown that this K^+ conductance is not distributed uniformly over the cell surface, but rather is localized to particular cell regions. In astrocytes of the salamander optic nerve, K^+ conductance is concentrated in the cells' endfeet, the bulbous enlargements at the ends of the cells' radial processes (Newman, 1986a). In the salamander, the membrane conductance of astrocyte endfeet is approximately 10-fold larger than the conductance of other regions of the cell (Newman, 1986a).

Potassium conductance is similarly localized over the surface of salamander Müller cells. Müller cells are the principal glial elements of the vertebrate retina. These radial cells possess many of the properties and functions of astrocytes. In the salamander, the membrane conductance of the Müller cell endfoot is roughly 57 times that of other cell regions (Newman, 1985a). Approximately 95% of the total conductance of salamander and frog Müller cells is localized to the endfoot (Newman, 1985a).

Glial cells are believed to regulate extracellular K^+ levels ($[K^+]_0$) in the CNS by, among other mechanisms, spatial buffering (Orkland et al., 1966). Current, in the form of K^+ flux, enters glial cells in regions of raised $[K^+]_0$. In order to maintain net electrical neutrality, an equal K^+ current flows out from other regions of these cells or from electrically coupled cells. The result of these spatial buffering currents is to transfer K^+ from regions where $[K^+]_0$ is high to regions where $[K^+]_0$ is low.

The strikingly nonuniform distribution of K^+ conductance that has been demonstrated in Müller cells and astrocytes has important implications for spatial buffering. Following an increase in $[K^+]_0$ and the influx of K^+ into glial cells, K^+ efflux occurs principally across the high-conductance endfoot membrane. This directed flow of spatial buffering current, termed "K^+ siphoning" (Newman et al., 1984), enhances the spatial buffering process. Excess K^+ generated by neuronal activity is siphoned from the retina and the brain into the large fluid reservoirs of the vitreous humor (Newman, 1985b) and CNS capillaries (Newman, 1986a).

To date, high endfoot conductance in glial cells has been demonstrated only in amphibians. It remains to be determined whether this membrane specialization is a general property of vertebrate glial cells or is restricted to glial cells of cold-blooded vertebrates. I address this issue in the present study, where I have determined the distribution of K^+ conductance over the surface of mammalian Müller cells. Cells from species with vascularized and avascular retinas were studied. A preliminary report of some of these results has appeared previously (Newman, 1986b).

Materials and Methods

Animals. The following species were used in the study: tiger salamanders (*Ambystoma tigrinum*, aquatic stage), black Hartley guinea pigs, dutch belted rabbits, pigmented mice (C57BL), cats, and one owl monkey (*Aotus trivirgatus*).

Anesthesia and death of animals. Salamanders were killed by decap-

Received Sept. 26, 1986; revised Dec. 17, 1986; accepted Feb. 6, 1987.

I thank Stephen P. Bartels for providing the retinal tissue of the owl monkey and Janice I. Gepner, Peter H. Hartline and an anonymous reviewer for their helpful comments on the manuscript. This work was supported by NIH Grant EY 04077.

Correspondence should be addressed to the author at Eye Research Institute of Retina Foundation, 20 Staniford Street, Boston, MA 02114.

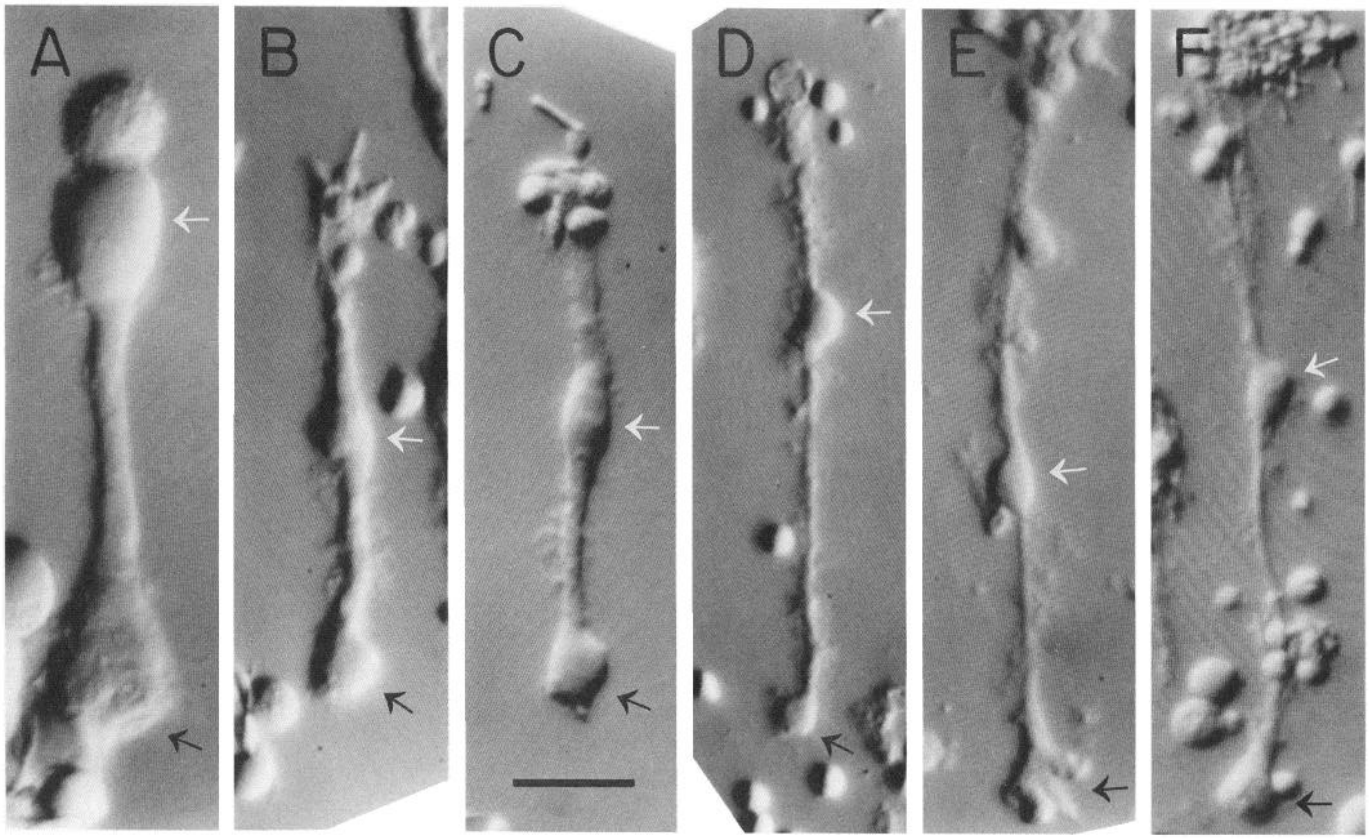

Figure 1. Photomicrographs of freshly dissociated Müller cells isolated from the retinas of (*A*) tiger salamander, (*B*) rabbit, (*C*) guinea pig, (*D*) mouse, (*E*) owl monkey, and (*F*) cat. Cell somata are indicated by *white arrows* and cell endfeet by *black arrows*. The distal (photoreceptor) ends of the cells are at the *top*. The cells are all shown at the same magnification. Scale bar, 20 μm.

itation and pithing. The eyes were then enucleated. Mice were killed by cervical dislocation and decapitation and then enucleated. Guinea pigs, rabbits, and cats were anesthetized by intramuscular injection of xylazine (40, 50, and 7.5 mg/kg, respectively) and ketamine (200, 250, and 35 mg/kg, respectively). The eyes were enucleated and the animals killed by injection of pentobarbital into the heart. The monkey was deeply anesthetized by intramuscular injection of pentobarbital (12 mg/kg), enucleated, and killed by pentobarbital overdose.

Solutions. All Ringer's solutions were buffered to pH 7.4 with bicarbonate and 5% CO_2. Normal mammalian Ringer's contained (in mM): NaCl, 116; KCl, 5; $CaCl_2$, 1.8; $MgSO_4$, 0.8; NaH_2PO_4, 0.5; $NaHCO_3$, 26; and dextrose, 10. $CaCl_2$ and $MgSO_4$ were omitted from Ca^{2+}-, Mg^{2+}-free (CMF) Ringer's. The composition of the salamander Ringer's solutions was the same except that the NaCl and KCl concentrations were (in mM): NaCl, 80; KCl, 2.5.

Recording (suction) electrodes were filled with 156 mM KCl (for mammals) and 125 mM KCl (for salamanders). For mammalian experiments, K^+ ejection pipettes were filled with a solution containing (in mM): NaCl, 97.5; KCl, 50; $CaCl_2$, 1.8; $MgSO_4$, 0.8; HEPES, 10, adjusted to pH 7.4. The composition of the salamander K^+ ejection solution was the same except that the NaCl and KCl concentrations were (in mM): NaCl, 84; KCl, 25. Recording electrode and ejection pipette solutions had the same osmolarity as the Ringer's solution appropriate for each species.

Cell dissociation. All Müller cell recordings were made from freshly dissociated cells. A modification of the dissociation procedures of Newman (1985a) and Sarthy and Lam (1978) was used. For all species, pieces of retinal tissue were isolated from the posterior hemisphere of the eye, avoiding the region of the optic disc and, in rabbits, the visual streak and myelinated rays. In cats, retinal tissue overlying the tapetum was used. In a separate series of experiments on cat, retinal tissue from the far periphery (bordering the ora serrata) was used.

Pieces of isolated retina were rinsed in CMF Ringer's and then incubated in CMF Ringer's containing papain (0.5 mg/ml; Cooper Biomedical, No. 3126) and cysteine (10 mM) for 30 min at 36°C (30°C for salamanders). The retinal tissue was rinsed twice in normal Ringer's containing 0.1% BSA (Sigma; No. A-4378) and then triturated in Ringer's containing 0.1% BSA and 0.01% DNAase (Sigma; No. D-0876).

Cell recording. The procedures used to record from dissociated Müller cells have been described previously (Newman, 1985a). Briefly, dissociated cells were placed in a perfusion chamber and allowed to settle on a concanavalin A-coated microscope slide. The cells were continually perfused with Ringer's bubbled with 5% CO_2 and 95% O_2. Recordings were made within 4 hr of cell dissociation.

Whole-cell recordings were made with suction electrodes filled with a KCl solution of the same osmolarity as the external bathing solution. Recordings were always made from the cell soma. After a high-resistance seal was obtained, the membrane beneath the recording electrode was ruptured to achieve whole-cell recording.

In preliminary recordings made from salamander and mouse cells, suction electrodes were filled with a KCl solution buffered with EGTA to achieve a 10^{-8} mM Ca^{2+} concentration. Results were similar to those obtained with the standard (unbuffered) recording solution, except that the addition of EGTA appeared to hasten the deterioration of a cell once the membrane patch was ruptured.

The input resistance of Müller cells was determined by passing 50–100 pA depolarizing current pulses through the recording electrode. Measurements were corrected for the voltage drop across the access resistance of the electrode.

Recording temperature. Cells were maintained at approximately 15°C for the duration of an experiment. In preliminary experiments, recordings were made from mouse and rabbit Müller cells at 31–35°C. There were no significant differences between the responses recorded at the higher temperatures and those recorded at 15°C. However, cell recordings and the general appearance of the dissociated cells declined much more rapidly at 31–35°C.

Micrographs. Cells were viewed through Nomarski optics, a 20 times magnification, ultralong working distance objective (Olympus; ULWD-CDplan 20), and a video system. They were photographed from the face of a video monitor.

Results

The distribution of K^+ conductance over the surface of Müller cells was determined for 5 mammalian species—guinea pig, rabbit, mouse, monkey, and cat—and for salamander, which provided a useful comparison to the mammalian species.

Morphology

Photomicrographs of freshly dissociated Müller cells of these 6 species are shown in Figure 1. The cells are all illustrated at the same magnification. Cell somata are indicated by white arrows and cell endfeet by black arrows.

All of these Müller cells had similar morphological features. Radiating from the soma (located in the inner nuclear layer of the retina *in situ*) was a proximal process that projected through the inner plexiform layer *in situ* (downwards from the cell somata in the photographs). The proximal process was terminated by a single endfoot, which lay against the inner limiting membrane *in situ*. A distal process, passing through the outer plexiform layer and the outer nuclear layer *in situ*, also projected from the soma (upwards in the photographs). The distal end of this process lay at the level of the outer limiting membrane *in situ*.

Systematic differences were noted between Müller cells of the various mammalian species. Müller cells from the vascularized retinas of the mouse, monkey, and cat (Fig. 1, *D–F*) were longer and much thinner than cells from the avascular retinas of the rabbit and guinea pig (Fig. 1, *B, C*). The distal processes of mouse, monkey, and cat cells, in contrast to cells of the rabbit and guinea pig, were often branched and were covered with fine extensions.

Monkey Müller cells (Fig. 1*E*) differed from those of all other species in several respects. Only in monkey cells was the distal process longer than the proximal process. Also, the endfeet of monkey cells had a unique morphology. Instead of having a single bulbous enlargement, monkey endfeet were often composed of flattened, fingerlike projections 5–10 μm long (see Figs. 1*E*, 4).

The dissociation procedure described in Materials and Methods often resulted in isolated Müller cells with extraneous cell bodies and other cell debris attached (Fig. 1, *B, C, E, F*). A more vigorous dissociation treatment (a higher papain concentration or a longer enzyme incubation period) resulted in cleaner Müller cells (see Reichenbach and Wohlrab, 1986). However, this stronger treatment damaged the cells, as was evidenced by lower cell resting potentials.

Electrophysiology

The resting membrane potential (E_m) and input resistance values for Müller cells of the 6 species are given in Table 1. For each species, E_m was close to the value of the K^+ equilibrium potential (E_K), indicating that the cell membrane was almost exclusively permeable to K^+. E_K can be calculated precisely because the internal K^+ concentration ($[K^+]_i$) was equal to the $[K^+]$ within the recording suction electrode. Note that both E_m and E_K were more negative for salamander cells than for mammalian cells because of $[K^+]$ differences in the external and internal solutions.

If one assumes that mammalian Müller cells are permeable only to K^+ and Na^+, as appears to be the case for salamander Müller cells (Newman, 1985a), the ratio of K^+ to Na^+ permeabilities (p_K/p_{Na}) can be calculated from the Goldman equation (Goldman, 1943). The calculated p_K/p_{Na} ratio for each species is given in Table 1. These permeability ratios ranged from 71.1 in cat Müller cells of the peripheral retina to 114.1 in monkey cells. These values are larger than the p_K/p_{Na} permeability ratio of 27.0 measured in dissociated turtle Müller cells (Conner et al., 1985), but are not as large as the p_K/p_{Na} ratio of 490 measured in salamander Müller cells *in situ* (Newman, 1985a). It is likely that the dissociation procedure makes the membrane of Müller cells somewhat less selective for K^+. The permeability ratio calculations were based on the following ion concentrations (in mM): mammals, $[K^+]_0 = 5$; $[K^+]_i = 156$; $[Na^+]_0 = 116$; $[Na^+]_i = 0$. Salamander, $[K^+]_0 = 2.5$; $[K^+]_i = 125$; $[Na^+]_0 = 82.5$; $[Na^+]_i = 0$.

Table 1. Electrical parameters of dissociated Müller cells

Species	(No. of cells)	E_m (mV)	E_K (mV)	p_K/p_{Na}	Resistance (MΩ)
Salamander	(23)	−89.3	−98.5	74.5	9.7
		(0.5)			(0.8)
Guinca pig	(15)	−80.8	−86.7	88.6	8.0
		(0.7)			(0.6)
Rabbit	(18)	−79.7	−86.7	72.9	21.5
		(1.5)			(1.5)
Mouse	(11)	−81.7	−86.7	106.6	14.6
		(0.4)			(1.1)
Monkey	(17)	−82.0	−86.7	114.1	10.5
		(0.3)			(1.1)
Cat (central)	(10)	−80.7	−86.7	86.9	3.9
		(0.4)			(0.6)
Cat (peripheral)	(5)	−79.6	−86.7	71.7	7.8
		(1.0)			(2.5)

Mean values (±SEM in parentheses) of the membrane resting potential (E_m), K^+ equilibrium potential (E_K), ratio of K^+ permeability to Na^+ permeability (p_K/p_{Na}), and input resistance (Resistance) of Müller cells for the 6 species tested. See text for details.

Potassium conductance distribution

The distribution of K^+ conductance over the surface of dissociated Müller cells was determined by monitoring cell depolarizations evoked by focal increases in $[K^+]_0$. This method has been described in detail elsewhere (Newman, 1985a). In brief, the cell membrane potential was monitored with a suction electrode attached to the soma while a high-molarity K^+ solution was pressure-ejected onto discrete regions of the cell surface. The local increase in $[K^+]_0$ produced by the K^+ ejection evoked a cell depolarization that was recorded in the soma.

In some cases, K^+ was ejected into a mass of cell debris loosely attached to the surface of Müller cells, instead of onto the bare cell surface. This did not noticeably influence K^+ response measurements, as evidenced by the fact that responses to K^+ ejections directed at regions covered with cell debris had similar magnitudes and time courses to responses evoked by K^+ ejections directed towards adjacent regions of bare membrane.

In a typical experiment, K^+ responses were measured at 8 standard locations across the surface of an isolated Müller cell. These locations are illustrated in Figures 2–4 and are labeled as follows: *A*, endfoot; *B*, proximal end of proximal process; *C*, midway along proximal process; *D*, distal end of proximal process; *E*, soma; *F*, proximal end of distal process; *G*, midway along distal process; and *H*, distal end of the cell.

Salamander. The responses of a dissociated salamander Mül-

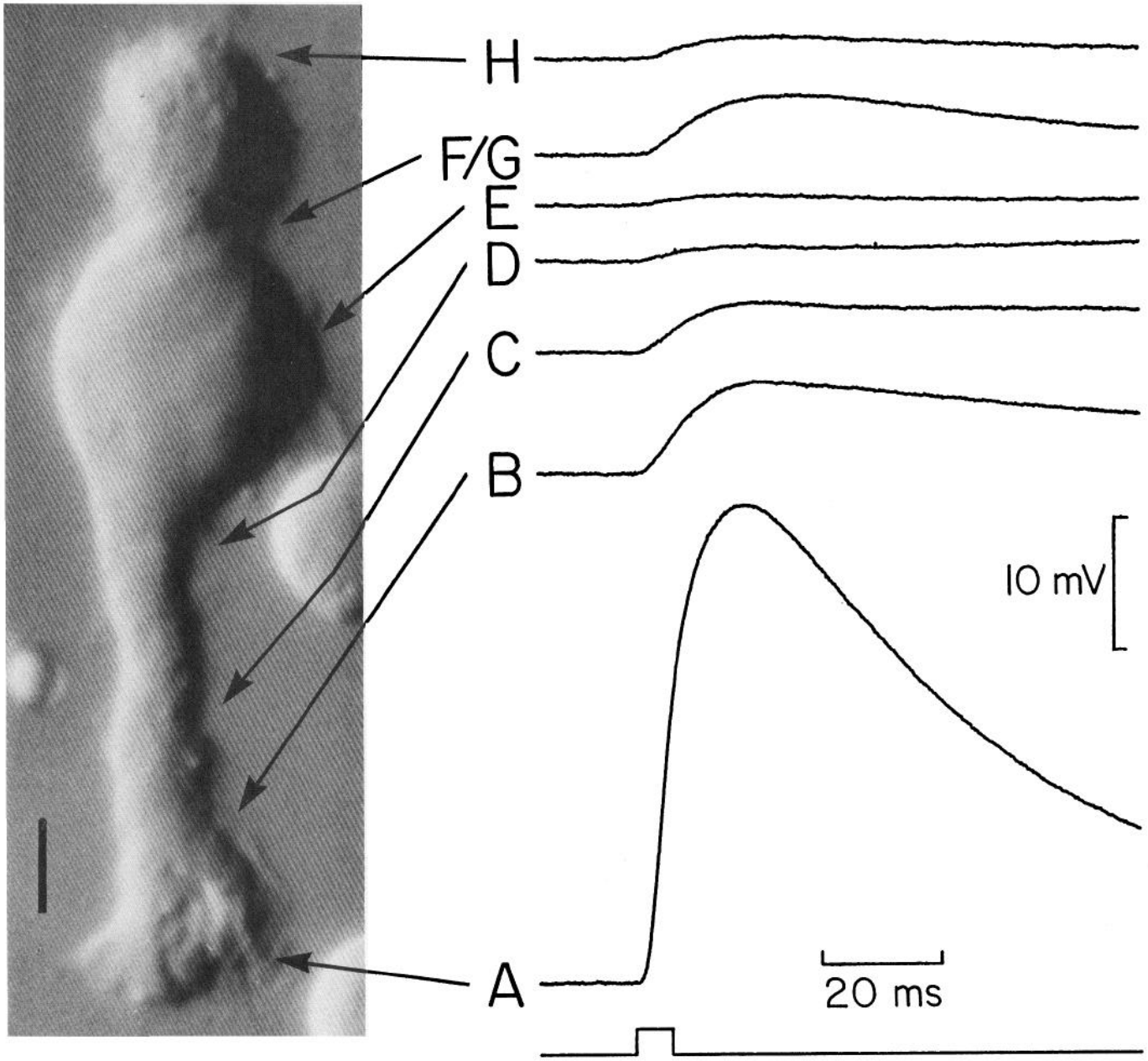

Figure 2. Voltage responses of a dissociated salamander Müller cell to focal K^+ ejections. Responses were recorded from the *cell at the left.* Sites of K^+ ejection are indicated in the photograph. These locations are typical of the ejection sites used in K^+ ejection experiments on all 6 species: *A,* Endfoot. *B,* Proximal end of proximal process. *C,* Midway along proximal process. *D,* Distal end of proximal process. *E,* Soma. *F,* Proximal end of distal process. *G,* Midway along distal process. *H,* distal end of cell. In salamander cells, only one ejection site was used along the distal cell process and was labeled (*F/G*). The onset and duration of the K^+ ejection pressure pulse is indicated below trace *A*. Scale bar, 10 μm.

ler cell to a series of K^+ ejections are illustrated in Figure 2. When K^+ was ejected onto the endfoot (Fig. 2*A*), a large, transient depolarization was recorded in the soma. If the ejection pipette was moved just 13 μm to the proximal end of the proximal process (Fig. 2*B*), the evoked response was much smaller. Ejections directed at other sites across the surface of the cell resulted in even smaller responses. However, the K^+ response of the distal cell process (Fig. 2*F/G*) was significantly larger than the responses of adjacent regions. (Because the distal processes of salamander Müller cells were so short, the proximal and middle sites along this process, sites *F* and *G*, could not be distinguished. Only one ejection site, designated *F/G*, was tested.)

Mammals. The responses of dissociated rabbit Müller cells to a series of K^+ ejections were similar, in many respects, to those recorded from salamander cells. As in salamanders, a K^+ ejection directed towards the endfoot (Figure 3*A*) produced a significantly larger response than did ejections directed towards other cell regions (Fig. 3, *B–H*). However, the K^+ endfoot response of rabbit Müller cells did not dominate over the responses of other cell regions to the extent that it did in salamanders. Ejections directed towards the distal end of the cell (Fig. 3, *G, H*) produced larger responses than did ejections directed towards other cell regions (Fig. 3, *B–F*).

The K^+ ejection responses recorded from monkey Müller cells differed substantially from the results obtained with salamander and rabbit cells. Potassium ejection responses of the endfoot

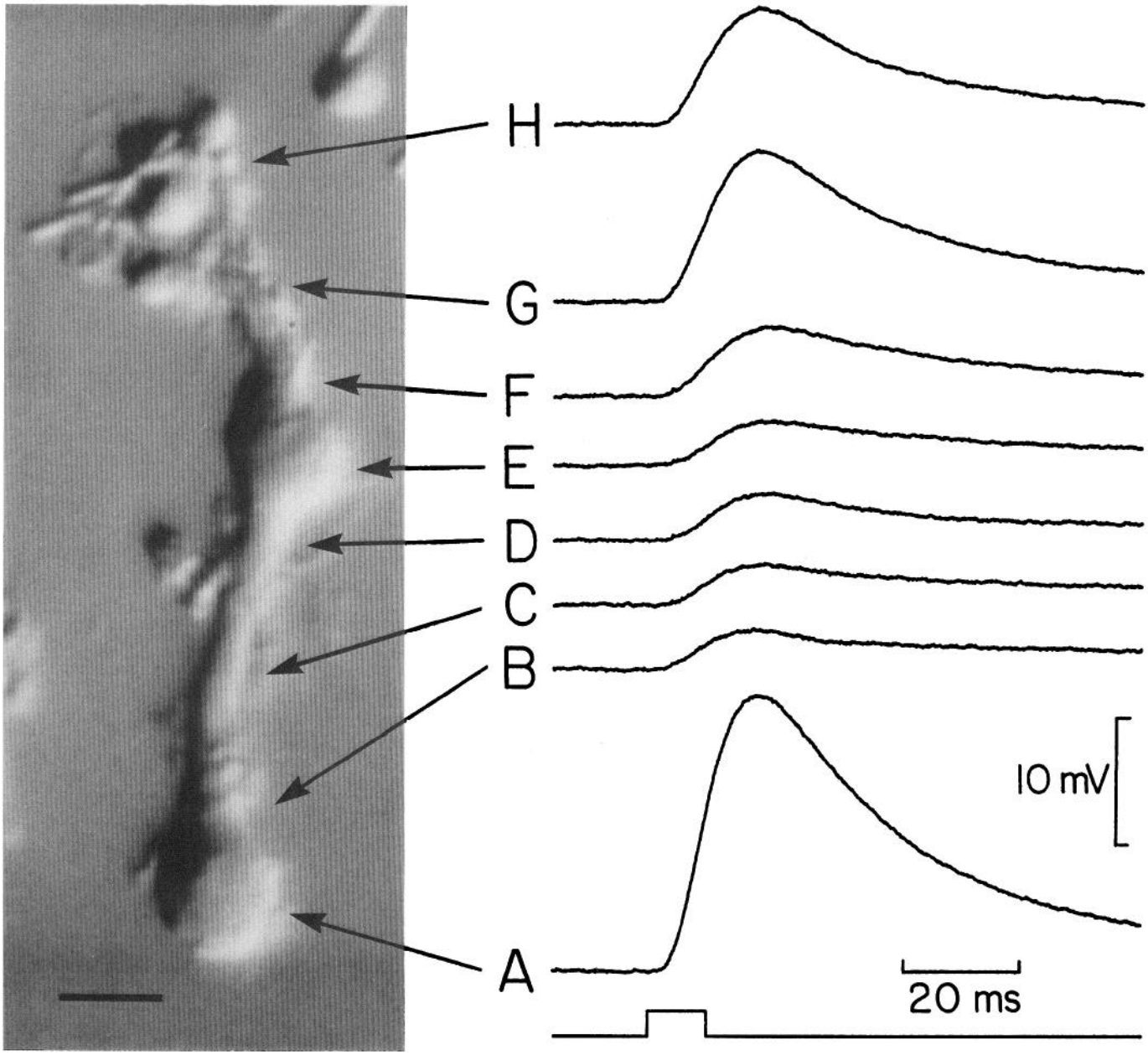

Figure 3. Voltage responses of a dissociated rabbit Müller cell to focal K^+ ejections. See Figure 2 for details. Scale bar, 10 μm.

(Fig. 4*A*) were larger than the responses of the proximal process (Fig. 4, *B–D*), as they were in salamander and rabbit. However, the responses of the soma (Fig. 4*E*) and the distal process (Fig. 4, *F–H*) either exceeded or were roughly equal to the endfoot response.

Potassium ejection-response summary. Potassium ejection experiments similar to the ones illustrated in Figures 2–4 were conducted on a series of Müller cells from each of 6 species: salamander, rabbit, guinea pig, mouse, monkey, and cat. The results of these experiments are summarized in Table 2 and are shown graphically in Figure 5. For each cell that was monitored, K^+ ejection-response magnitudes were expressed as a percentage of the endfoot response of that cell. The results shown in Table 2 and Figure 5 are the means of these normalized response values.

Central and peripheral cat Müller cells. The morphology of Müller cells differed significantly among the 6 species used in this study (see Fig. 1). In many species, cell morphology also varies considerably between different retinal regions of a single species (Reichenbach and Wohlrab, 1986). For example, Figure 6 shows one Müller cell isolated from the posterior hemisphere of the cat retina (Fig. 6*A*) and one cell isolated from the far periphery of the retina, near the ora serrata (Fig. 6*B*). The peripheral retina is thinner than the central retina, and cells isolated from the periphery are considerably shorter than those isolated from the posterior hemisphere.

The membrane properties of these 2 groups of cat Müller cells were investigated in a series of experiments. Cells were classified as peripheral if they were less than 100 μm long and were isolated from the peripheral retina, or as central if they were greater than

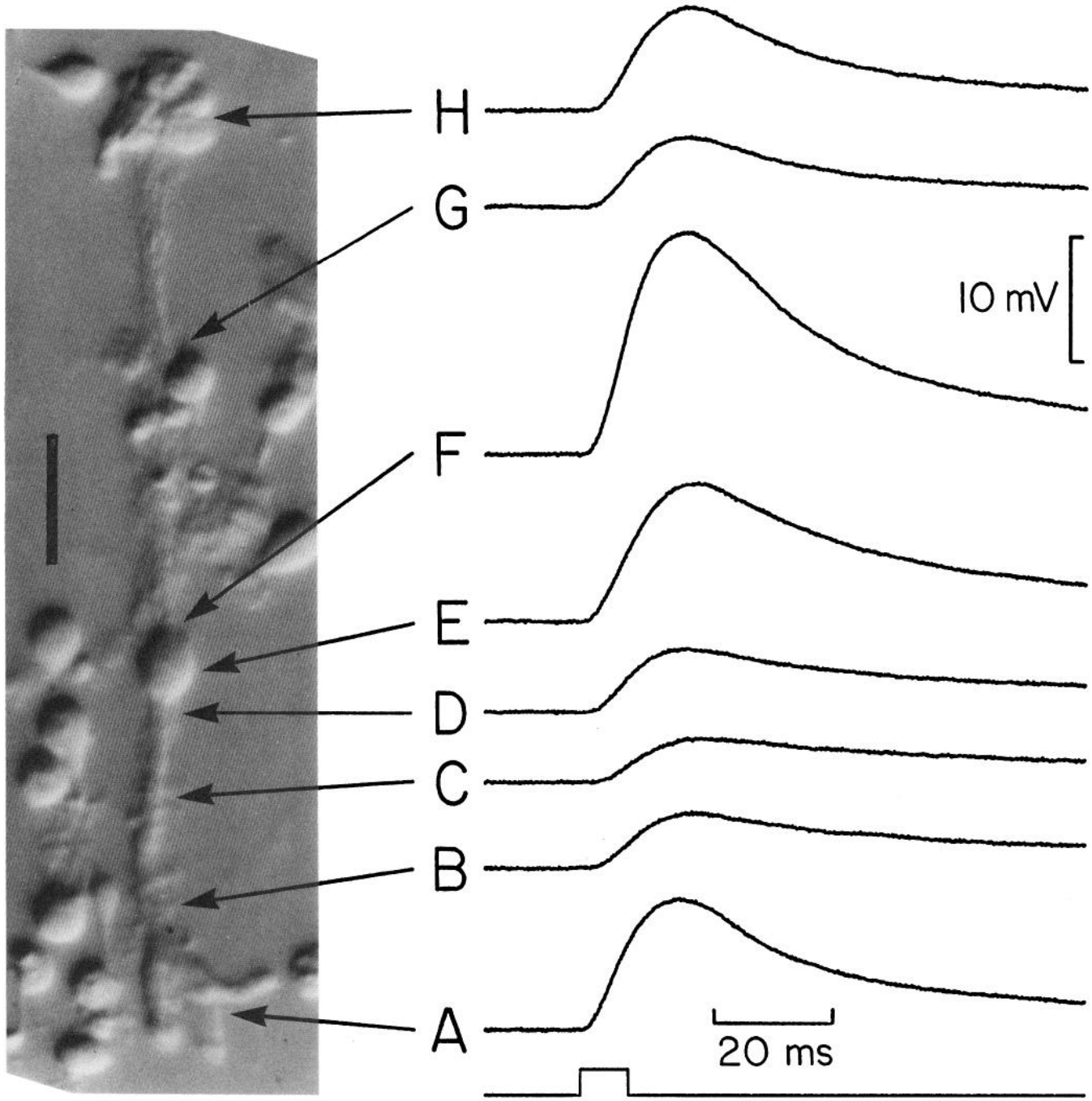

Figure 4. Voltage responses of a dissociated monkey Müller cell to focal K^+ ejections. See Figure 2 for details. Scale bar, 20 μm.

or equal to 125 μm long. As shown in Table 1, mean resting potentials were similar for the 2 groups: central, −80.7 mV; peripheral, −79.6 mV. On the other hand, the input resistance of the 2 groups differed by a factor of 2: central, 3.9 MΩ; peripheral 7.8 MΩ.

The responses of these 2 types of cat Müller cells to a series of K^+ ejections also differed. As is summarized in Table 2 and shown in Figure 7, the responses of the soma and portions of the proximal and distal processes of peripheral Müller cells (sites *D–G*) were significantly smaller than the corresponding responses of central cells.

Discussion

Measurement of regional K^+ conductance

The distribution of K^+ conductance over the surface of Müller cells can be determined from the relative magnitudes of response to K^+ ejections, such as those measured in this study. As demonstrated previously (Newman, 1985a), the magnitude of a cell response to a K^+ ejection is directly proportional to the total K^+ conductance of the cell membrane exposed to the $[K^+]_o$ increase. Note well that this method does *not* measure the specific membrane conductance of a cell region. Rather, the mag-

nitude of a K^+ ejection response is proportional to the *total* K^+ conductance of a region, i.e., the specific conductance *times* the total surface area of that region. This quantity may be termed the "regional K^+ conductance," to distinguish it from the specific K^+ conductance of a region. All references to measured conductances in this paper must be understood in terms of regional conductances, not specific conductances.

The concept of regional K^+ conductance is quite useful when considering the function of Müller cells. For example, local increases in $[K^+]_o$ produced by neuronal activity induce K^+ currents within Müller cells (spatial buffer currents). These currents, in turn, help to reduce the original $[K^+]_o$ increase and to generate field potentials (see below). The magnitude of the K^+ current flowing through Müller cells is determined, in large part, by the regional K^+ conductance of that portion of the cell exposed to the $[K^+]_o$ increase (Newman et al., 1984; Brew and Attwell, 1985).

Conductance distribution in mammalian cells

The principal finding of this study is that Müller cells of mammalian species, like those of amphibians, possess strikingly nonuniform distributions of K^+ conductance over their cell surface. The K^+ conductance distributions varied considerably among the 6 species tested, as can be appreciated by referring to Figure 5. Despite these variations, however, some general patterns in conductance distribution can be found.

The most significant variation in the K^+ conductance distribution among the 6 species was in the conductance in the middle portion of the cell (Fig. 5, *D–F*), which corresponds to the cell region lying within the inner nuclear layer *in situ*. In all 3 species with avascular retinas—salamander, rabbit, and guinea pig—the conductance within this region never exceeded 28.9% of the endfoot conductance. On the other hand, in mouse and monkey, both of which have vascularized retinas, the maximal conductance within the middle portion of the cell was 129.8 and 125.5% of the endfoot conductance, respectively. The K^+ conductance distribution of the cat, which also has a vascularized retina, differed substantially from those of all other species tested. On the whole, however, the conductance distribution of the cat more closely resembled those of the 2 other vascularized species. Thus, despite individual variations (most notably, the cat), the general impression conveyed by the summary plots in Figure 5 is that Müller cell conductance distributions fall into 1 of 2 general patterns, i.e., vascular or avascular.

The K^+ conductance of the distal end (site *H*) of Müller cells also differed among the species tested. The conductance of the

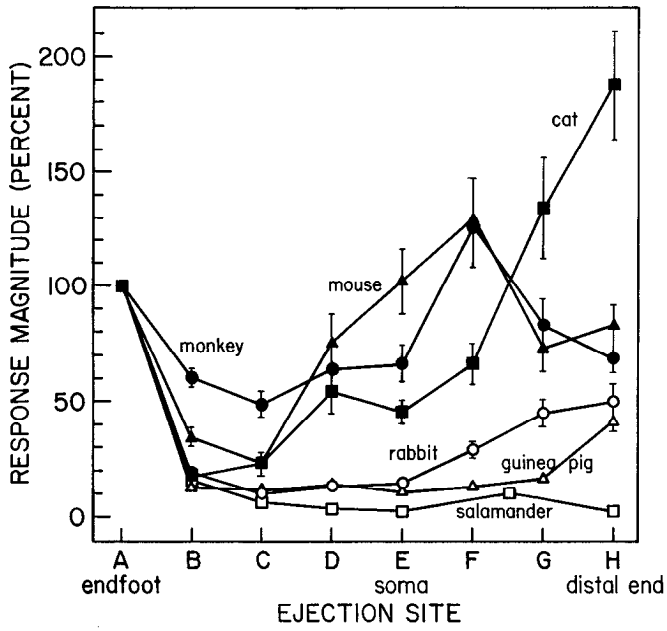

Figure 5. Summary of voltage responses to K^+ ejections recorded from dissociated Müller cells of tiger salamander (□), rabbit (○), guinea pig (△), mouse (▲), owl monkey (●), and cat (■; central retina). Values represent the mean ± SEM of individual responses, which are expressed as a percentage of the endfoot response of each cell. Ejection site locations are indicated along the abscissa (see Fig. 2).

Table 2. Voltage-response magnitudes of dissociated Müller cells to focal K^+ ejections

		K^+ ejection site							
			Proximal process				Distal process		
Species	(No. of cells)	Endfoot A	Proximal B	Mid C	Distal D	Soma E	Proximal F	Mid G	End H
Salamander	(25)	100.0	15.7	6.2	3.5	2.4	10.3	10.3	2.4
			(1.9)	(0.2)	(0.3)	(0.2)	(1.0)	(1.0)	(0.3)
Guinea pig	(15)	100.0	12.6	11.4	14.0	10.6	13.0	16.4	41.2
			(0.9)	(1.0)	(1.2)	(0.9)	(1.8)	(2.2)	(4.0)
Rabbit	(14)	100.0	19.2	9.9	13.1	14.6	28.9	44.9	49.8
			(2.2)	(1.1)	(1.6)	(2.0)	(3.8)	(6.0)	(8.3)
Mouse	(15)	100.0	34.3	23.1	75.5	102.1	129.8	72.9	82.9
			(4.8)	(5.0)	(12.8)	(14.4)	(18.4)	(10.1)	(9.0)
Monkey	(13)	100.0	60.2	48.5	63.9	66.1	125.5	82.7	68.3
			(4.5)	(6.1)	(6.4)	(8.2)	(17.7)	(11.8)	(6.0)
Cat (central)	(11)	100.0	17.4	23.0	54.1	45.3	66.1	133.8	187.1
			(3.1)	(4.1)	(9.4)	(5.3)	(8.9)	(22.1)	(23.6)
Cat (peripheral)	(6)	100.0	17.3	20.4	29.7	27.0	31.8	58.2	200.2
			(2.6)	(2.8)	(4.7)	(4.3)	(6.1)	(9.0)	(29.0)

Values represent the means (±SEM in parentheses) of individual K^+ responses, expressed as a percentage of the endfoot response of each cell. Data are shown graphically in Figures 5 and 7.

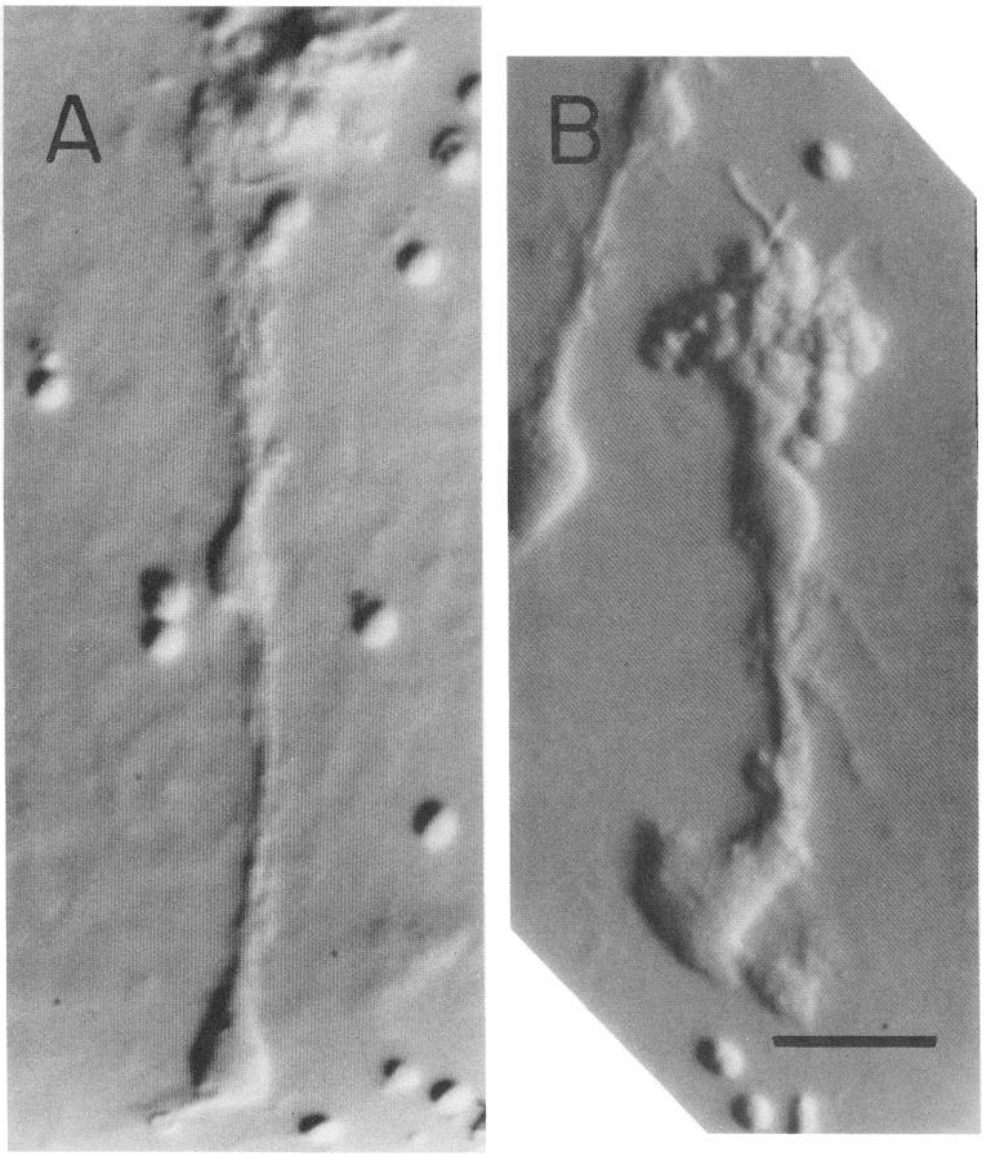

Figure 6. Photomicrographs of dissociated cat Müller cells isolated from (*A*) the central retina (posterior hemisphere) and (*B*) the peripheral retina. The 2 cells are shown at the same magnification. Scale bar, 20 μm.

distal end of all 5 mammalian species, unlike that of the salamander, was a significant fraction of the endfoot conductance. Again, the cat differed from all other species in having a distal end conductance that was twice the endfoot value.

The division of Müller cells into 2 classes, those from vascular and those from avascular retinas was supported by the results obtained from central and peripheral cat Müller cells. The central region of the cat retina is well vascularized (Michaelson, 1954; Henkind, 1966), while the extreme periphery of the retina is poorly vascularized or avascular (Toussaint et al., 1961; Hogan et al., 1971). As illustrated in Figure 7, conductance values within the middle region (Fig. 7, *D–F*) of cat Müller cells from the central retina were significantly larger than were the corresponding conductances of cells from the peripheral retina. Thus, the K^+ conductance distribution of cat Müller cells from the central (well-vascularized) retina more closely resembled the "vascular" type than did the conductance distribution of cells from the peripheral (poorly vascularized) retina.

In vascularized species, the blood vessels of the deep retina are completely surrounded by Müller cell processes (Hogan and Feeney, 1963; Kuwabara, 1969; Hogan et al., 1971). These vessels lie within or at the borders of the inner nuclear layer (Michaelson, 1954; Toussaint et al., 1961), which corresponds to the region of high conductance in mouse and monkey Müller cells (sites *D* through *F*). Although this correspondence does not provide direct evidence, it suggests that those regions of Müller cells in direct contact with blood vessels may have high K^+ conductance. This would be analogous to the situation in astrocytes, where the endfeet, which surround the blood vessels of the brain, have a much higher K^+ conductance than do other cell regions (Newman, 1986a).

Function of K^+ conductance distributions in mammals

The classification of Müller cells according to whether they are from vascular or avascular species suggests a possible function for the observed distributions of K^+ conductance. Müller cells are believed to regulate $[K^+]_o$ in the retina by means of spatial buffering (Newman, 1985b). In avascular retinas, the most effective place to store excess K^+ generated by neuronal activity is in the vitreous humor. In order to transfer K^+ to the vitreous

by spatial buffering, the conductance of the endfoot of Müller cells must be larger than the conductance of other cell regions (Newman et al., 1984). This is the distribution found in Müller cells of the salamander, rabbit, and guinea pig, all avascular species.

In vascularized retinas, on the other hand, it may be more profitable to transfer a portion of the excess K^+ into retinal capillaries instead of into the vitreous. As suggested above, the data from mouse and monkey cells are consistent with the possibility that Müller cell processes in contact with capillaries have high conductances. If this proved to be the case, then a substantial fraction of the K^+ transferred by spatial buffer currents in Müller cells would be deposited on the ablumenal walls of retinal capillaries. This K^+ would not diffuse passively into the blood because capillary endothelial cells in the CNS are largely impermeable to K^+ (Hansen et al., 1977). However, the K^+ could be actively transported into the blood by the Na^+/K^+ ATPase located on the ablumenal face of capillary endothelial cells (Betz et al., 1980).

Conductance of the endfoot. Although K^+ conductance was greatest in the middle and distal portions of Müller cells of vascularized species, the conductance of the endfoot in 2 of these species (mouse and monkey) was still larger than the conductance of most other cell regions. It is likely that a significant fraction of the K^+ transported by spatial buffer currents in these 2 species is siphoned from the endfoot. In vascularized species, Müller cell endfeet terminate on blood vessels at the retinal surface, as well as onto the inner limiting membrane (Karschin et al., 1986). Thus, the K^+ siphoned from these endfeet may be directed into the blood, as well as into the vitreous humor.

Cat Müller cells. The distribution of K^+ conductance in cat Müller cells differed substantially from those of the 2 other vascularized species. The conductance of the distal end of cat Müller cells (both central and peripheral) was double that of the endfoot. Thus, a much smaller fraction of spatial buffer current would be expected to flow from the endfoot in this species, i.e., a smaller fraction of excess K^+ is siphoned into the vitreous.

The functional significance of the conductance distribution in cat Müller cells is not known. One could speculate that excess K^+ is siphoned from the distal end of these cells into the subretinal space surrounding the photoreceptors. Potassium siphoned into the subretinal space might then be transferred across the retinal pigment epithelium by spatial buffer currents (Immel and Steinberg, 1986) and into the choroidal circulation. Alternately, the high conductance of the distal end of cat Müller cells might aid in buffering the large $[K^+]_0$ decrease produced by rod photoreceptors (Steinberg et al., 1980).

Conductance distribution in salamander cells

The K^+ ejection results confirm the findings of earlier studies (Newman, 1984, 1985a) that demonstrated that the endfoot of salamander Müller cells had a far larger K^+ conductance than did other cell regions. Not previously reported is the finding that the conductance of the distal process of salamander Müller cells (Fig. 2*F/G*) is larger than the conductance of neighboring cell regions (it was 4.3 times greater than the conductance of the soma). The distal process of salamander cells was not tested in the earlier studies.

Generation of field potentials

Potassium spatial buffer currents flowing through Müller cells are believed to generate several components of the electroretinogram (ERG), including the b-wave, the M-wave, and the slow PIII response. The distribution of K^+ conductance across the surface of Müller cells determines, in large part, the polarity and magnitude of the potentials generated by these currents.

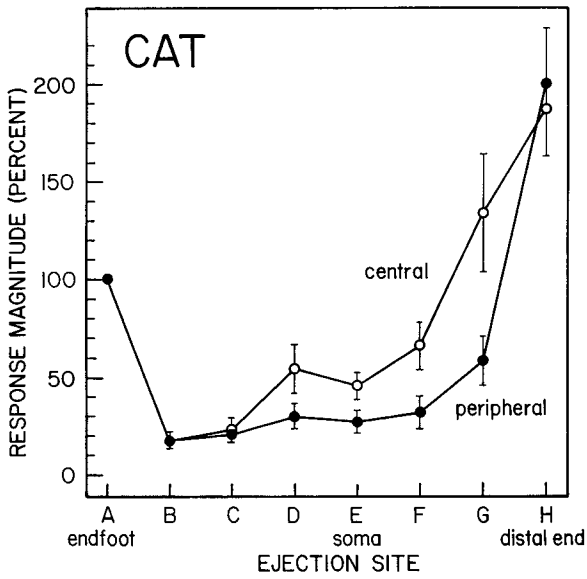

Figure 7. Summary of voltage responses (±SEM) to K^+ ejections recorded from dissociated cat Müller cells isolated from the central retina (○) and from the peripheral retina (●). Responses to ejections directed towards sites *D–G* are significantly smaller for peripheral cells than for central cells. See Figure 5 for details.

b-Wave. In amphibians and fish, the b-wave of the ERG is thought to be generated by light-evoked $[K^+]_0$ increases in the inner and outer plexiform layers (Miller and Dowling, 1970; Kline et al., 1978; Newman and Odette, 1984). Potassium currents generated by these two $[K^+]_0$ increases, which are preferentially shunted through Müller cell endfeet (Newman, 1980), give rise to vitreal-positive retinal potentials.

Because the distribution of K^+ conductance differs between vascularized mammalian species and amphibians, the pattern of intraretinal b-wave currents would also be expected to differ. In vascularized mammals, the current generated by the $[K^+]_0$ increase in the inner plexiform layer would be largely shunted out through the distal process of Müller cells, giving rise to a vitreal-*negative,* rather than *positive,* potential (see Kline et al., 1978). The current generated by the $[K^+]_0$ increase in the outer plexiform layer would also differ, although it is unclear whether the resulting potential would be enhanced or diminished as compared to amphibians.

M-wave. The M-wave is an intraretinally recorded negative potential originally described in amphibians (Karwoski and Proenza, 1977). It is generated by Müller cells in response to a light-evoked $[K^+]_0$ increase in the inner plexiform layer. Müller cells of vascularized retinas, because of their K^+ conductance distribution, should generate a negative transretinal M-wave. This has recently been confirmed in cat, where a vitreal-negative M-wave (Sieving et al., 1986a) and a negative scotopic threshold response (the scotopic equivalent of the M-wave; Sieving et al., 1986b) have been reported.

Slow PIII response. The slow PIII response is a transretinal, vitreal-negative potential believed to be generated by Müller cells in response to a slow $[K^+]_0$ decrease in the distal retina (Faber, 1969; Witkovsky et al., 1975). The magnitude of the

current generated by the $[K^+]_o$ decrease, as well as the amplitude of the resulting slow PIII potential, should depend on the conductance of the distal end of Müller cells. Thus, for a given $[K^+]_o$ decrease, one might expect cats to generate large, slow PIII responses and salamanders to generate small responses. (It may prove difficult to confirm this prediction because the generation of the slow PIII depends on several factors besides Müller cell conductance.)

Predictions

The results presented above demonstrate that, in the 6 species tested, the distribution of K^+ conductance over the surface of Müller cells depends largely on the pattern of retinal vascularization. This correlation raises the possibility that in avascular species, Müller cells siphon excess K^+ into the vitreous humor, whereas in at least some vascularized species (mouse and monkey), excess K^+ is siphoned into both the vitreous and retinal capillaries. The results lead to a number of predictions.

1. In vascularized species, excess K^+ generated by neuronal activity and siphoned by Müller cells into retinal capillaries should result in an increase in $[K^+]$ in the blood within the capillaries.

2. The processes of Müller cells in contact with retinal capillaries may be functionally and morphologically similar to the endfeet of glial cells. (Astrocyte endfeet directly contact brain capillaries.) These Müller cell processes should possess assemblies (orthogonal arrays of intramembrane particles) that are also found on Müller cell (Raviola, 1977) and astrocyte (Landis and Reese, 1974) endfeet.

3. The distribution of K^+ conductance in Müller cells of other species should follow the pattern observed in the present study. Müller cells of fish, reptiles, and birds, all of which have avascular retinas, should have K^+ conductance distributions similar to the cells of salamander, rabbit, and guinea pig.

4. The endfeet of amphibian Müller cells (Newman, 1985a), amphibian astrocytes (Newman, 1986a), and mammalian Müller cells (the present study) all have high K^+ conductance. The endfeet of mammalian astrocytes should also have high conductance.

References

Betz, A. L., J. A. Firth, and G. W. Goldstein (1980) Polarity of the blood–brain barrier: Distribution of enzymes between the luminal and antiluminal membranes of brain capillary endothelial cells. Brain Res. *192:* 17–28.

Brew, H., and D. Attwell (1985) Is the potassium channel distribution in glial cells optimal for spatial buffering of potassium? Biophys. J. *48:* 843–847.

Conner, J. D., P. B. Detwiler, and P. V. Sarthy (1985) Ionic and electrophysiological properties of retinal Müller (glial) cells of the turtle. J. Physiol. (Lond.) *362:* 79–92.

Faber, D. S. (1969) Analysis of slow transretinal potentials in response to light. Ph.D. thesis, State University of New York, Buffalo.

Goldman, D. E. (1943) Potential, impedance and rectification in membranes. J. Gen. Physiol. *27:* 37–60.

Hansen, A. J., H. Lund-Andersen, and C. Crone (1977) K^+-permeability of the blood–brain barrier, investigated by aid of a K^+-sensitive microelectrode. Acta Physiol. Scand. *101:* 438–445.

Henkind, P. (1966) The retinal vascular system of the domestic cat. Exp. Eye Res. *5:* 10–20.

Hogan, M. J., and L. Feeney (1963) The ultrastructure of the retinal vessels. III. Vascular–glial relationships. J. Ultrastruct. Res. *9:* 47–64.

Hogan, M. J., J. A. Alvarado, and J. E. Weddell (1971) *Histology of the Human Eye. An Atlas and Textbook,* Saunders, Philadelphia, PA.

Immel, J., and R. H. Steinberg (1986) Spatial buffering of K^+ by the retinal pigment epithelium in frog. J. Neurosci. *6:* 3197–3204.

Karschin, A., H. Wassle, and J. Schnitzer (1986) Immunocytochemical studies on astroglia of the cat retina under normal and pathological conditions. J. Comp. Neurol. *249:* 564–576.

Karwoski, C. J., and L. M. Proenza (1977) Relationship between Müller cell responses, a local transretinal potential, and potassium flux. J. Neurophysiol. *40:* 244–259.

Kettenmann, H., U. Sonnhof, and M. Schachner (1983) Exclusive potassium dependence of the membrane potential in cultured mouse oligodendrocytes. J. Neurosci. *3:* 500–505.

Kline, R. P., H. Ripps, and J. E. Dowling (1978) Generation of b-wave currents in the skate retina. Proc. Natl. Acad. Sci. USA *75:* 5727–5731.

Kuwabara, T. (1969) Blood vessels in the normal retina. In *The Retina: Morphology, Function and Clinical Characteristics,* B. R. Straatsma, M. O. Hall, R. A. Allen, and F. Crescitelli, eds., pp. 163–176, U. California P., Berkeley, CA.

Landis, D. M. D., and T. S. Reese (1974) Arrays of particles in freeze-fractured astrocytic membranes. J. Cell Biol. *60:* 316–320.

Michaelson, I. C. (1954) *Retinal Circulation in Man and Animals,* Charles C. Thomas, Springfield, IL.

Miller, R. F., and J. E. Dowling (1970) Intracellular responses of the Müller (glial) cells of mudpuppy retina: Their relation to b-wave of the electroretinogram. J. Neurophysiol. *33:* 323–341.

Newman, E. A. (1980) Current source-density analysis of the b-wave of frog retina. J. Neurophysiol. *43:* 1355–1366.

Newman, E. A. (1984) Regional specialization of retinal glial cell membrane. Nature *309:* 155–157.

Newman, E. A. (1985a) Membrane physiology of retinal glial (Müller) cells. J. Neurosci. *5:* 2225–2239.

Newman, E. A. (1985b) Regulation of extracellular potassium by glial cells in the retina. Trends Neurosci. *8:* 156–159.

Newman, E. A. (1986a) High potassium conductance in astrocyte endfeet. Science *233:* 453–454.

Newman, E. A. (1986b) Potassium conductance hot-spots in mammalian Müller (glial) cells. Soc. Neurosci. Abstr. *12:* 633.

Newman, E. A., and L. L. Odette (1984) Model of electroretinogram b-wave generation: A test of the K^+ hypothesis. J. Neurophysiol. *51:* 164–182.

Newman, E. A., D. A. Frambach, and L. L. Odette (1984) Control of extracellular potassium levels by retinal glial cell K^+ siphoning. Science *225:* 1174–1175.

Orkand, R. K. (1977) Glial cells. In *Handbook of Physiology. Sect. 1: The Nervous System,* J. M. Brookhart and V. B. Mountcastle, eds., pp. 855–875, American Physiological Society, Bethesda, MD.

Orkand, R. K., J. G. Nicholls, and S. W. Kuffler (1966) Effect of nerve impulses on the membrane potential of glial cells in the central nervous system of amphibia. J. Neurophysiol. *29:* 788–806.

Raviola, G. (1977) The structural basis of the blood–ocular barriers. Exp. Eye Res. *25*(Suppl.): 27–63.

Reichenbach, A., and F. Wohlrab (1986) Morphometric parameters of Müller (glial) cells dependent on their topographic localization in the nonmyelinated part of the rabbit retina. A consideration on functional aspects of radial glia. J. Neurocytol. *15:* 451–459.

Sarthy, P. V., and D. M. K. Lam (1978) Biochemical studies of isolated glial (Müller) cells from the turtle retina. J. Cell Biol. *78:* 675–684.

Sieving, P. A., L. J. Frishman, and R. H. Steinberg (1986a) M-wave of proximal retina in cat. J. Neurophysiol. *56:* 1039–1048.

Sieving, P. A., L. J. Frishman, and R. H. Steinberg (1986b) Scotopic threshold response of proximal retina in cat. J. Neurophysiol. *56:* 1049–1061.

Steinberg, R. H., B. Oakley II, and G. Niemeyer (1980) Light-evoked changes in $[K^+]_o$ in retina of intact cat eye. J. Neurophysiol. *44:* 897–921.

Toussaint, D., T. Kuwabara, and D. G. Cogan (1961) Retinal vascular patterns. Part II. Human retinal vessels studied in three dimensions. Arch. Ophthalmol. *65:* 575–581.

Walz, W., W. Wuttke, and L. Hertz (1984) Astrocytes in primary cultures: Membrane potential characteristics reveal exclusive potassium conductance and potassium accumulator properties. Brain Res. *292:* 367–374.

Witkovsky, P., F. E. Dudek, and H. Ripps (1975) Slow PIII component of the carp electroretinogram. J. Gen. Physiol. *65:* 119–134.